Reducing beam tracking complexity using a phase ramp and Fresnel lens when steering beams using spatial light modulators

Spaander, Joshua; Guo, Jian; Saathof, Rudolf; Gill, Eberhard

DOI
10.1364/OL.523438

Publication date
2024

Document Version
Final published version

Published in
Optics Letters

Optics Letters

Reducing beam tracking complexity using a phase ramp and Fresnel lens when steering beams using spatial light modulators

Joshua Spaander,* Jian Guo, Rudolf Saathof, and Eberhard Gill

Faculty of Aerospace Engineering, Delft University of Technology, Kluyverweg 1, 2629 HS Delft, The Netherlands
**j.j.spaander@tudelft.nl*

Received 14 March 2024; revised 31 May 2024; accepted 3 June 2024; posted 3 June 2024; published 21 June 2024

Steering multiple laser beams using spatial light modulators (SLMs) creates unwanted diffraction and reflections that are not modulated by the SLM, which can make beam tracking difficult. A novel, to the best of our knowledge, and simple beam steering methodology is proposed, which aims at reducing the influence of this clutter while maintaining tracking performance. The beam(s) are deliberately defocused before steering with a superposition of a phase ramp and Fresnel lens (PRFL) phase screen on the SLM. As a result, the non-modulated reflections and diffracted light are decreased in relative intensity to the steered beam, in turn allowing simple and standard peak intensity and center of gravity (CG) algorithms for tracking. Hardware demonstration shows tracking performance using the PRFL remained on-par with more complex filtering approaches while adding no additional hardware. This method has potential to improve the communication performance of multi-beam laser communication terminals.

https://doi.org/10.1364/OL.523438

Laser satellite communications require beam steering accuracy in the order of μrad, with kHz control bandwidth. As a result, beam tracking requirements are similarly stringent. This is no different in multi-beam laser satellite communications but applied to multiple beams. To control multiple beams, micromirror arrays (MMAs) and spatial light modulators (SLMs) are being considered as potential solutions. These devices can synthesize phase screens dynamically allowing for allocation steering surface area and unique steering angle to each beam [1]. Besides laser satellite communications, these devices are widely used for numerous other applications.

A drawback of these devices is that they act as diffraction gratings causing diffraction patterns, and non-modulated reflections form non-modulated beams (NMBs) [2–4]. These effects interfere with the intended image and could potentially compromise beam tracking [3]. Figure 1 shows an over-exposed image that illustrates these effects.

These effects can occur in a multi-beam steering control loop that uses an image detector to track beams together with an SLM or MMA to steer beams. The location determination of each beam needs to be determined accurately and fast enough to sustain high enough bandwidths for disturbance suppression. The presence of NMB and diffraction patterns could be particularly challenging, as these can be mistaken for communication beams in addition to the before mentioned drawbacks. To be able to perform multi-beam steering in such scenarios, algorithms are needed to filter out the incorrect beams. This increases complexity and required computational resources. Furthermore, the NMB and diffraction could couple into the wrong detector causing cross talk. These challenges could potentially become difficult to overcome, especially when the NMB and diffraction are higher in amplitude than the communication beams themselves. These drawbacks make SLMs as well as MMAs less attractive options for multi-beam steering.

The severity of diffraction and NMB is dependent on the SLMs or MMAs chosen. Namely, factors such as anti-reflection coatings, liquid crystal versus mirror based, and pixel size just to name a few, could affect the performance. However, these measures can come at high cost, lack availability, or are incompatible.

In literature, improvements in SLM beam steering has focused on optimizing phase ramp (PR) phase screens and filtering out the zeroth-order diffraction as well as non-modulated light through algorithms [3–8]. SLMs have also been used as lenses as part of optical steering systems and increasing its steering range limitations through optical design [9].

Instead, this work takes a different approach by separating the NMB from the modulated beam (MB) using the SLM itself. Using this novel approach, the influence of the NMB and diffraction is reduced by changing the diffraction pattern and relatively increasing the MB intensity through steering using the phase ramp and Fresnel lens (PRFL) super position phase screens shown in Fig. 2. As a way to assess the suitability of this new method, three criteria were considered:

(1) **Tracking can be done simply through peak intensity and center of gravity (CG) tracking.** If met, it reduces tracking complexity and/or increases reliability due to not having to resort to filtering.
(2) **The tracking error of the PRFL is the same or less than PR steering.** If met, it would imply that the implementation

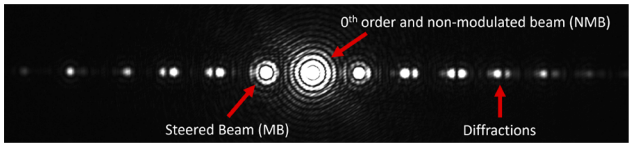

Fig. 1. Over-exposed image of an in-focus beam steered from the center slightly to the left, which shows the effect of the undesired reflections at the SLM. Note that the spots have different intensities, which is not obvious from the overexposure.

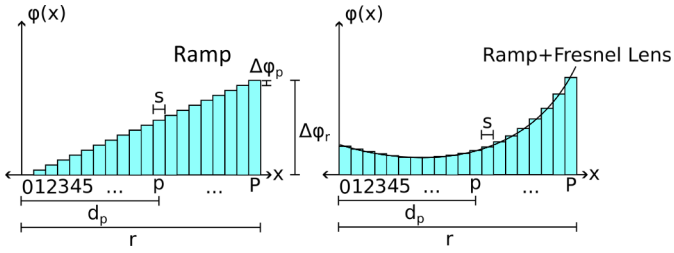

Fig. 2. Illustration of a phase ramp (PR) (left) and a phase ramp and Fresnel lens (PRFL) (right).

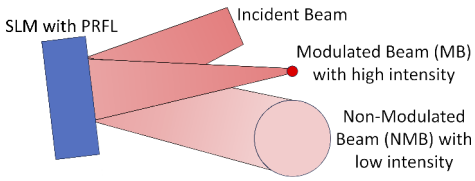

Fig. 3. Separation of the NMB and MB through the PRFL.

of the PRFL would not reduce the tracking performance and hence make it a potential candidate in a trade-off with PR.

(3) **Reduction of the diffraction patterns and NMB amplitude on the image detector.** If met, there could be a substantial reduction in cross talk in multi-beam receivers and clutter for multi-beam tracking. This in turn could potentially increase the number of beams which the system could accommodate.

In this method, separation and amplitude reduction of non-modulated light (which is the source of the NMB) from the modulated light is a key concept. Since the non-modulated light is not altered by the SLM, it can be separated by deliberately diverging/defocusing of the incident beam (just) before or after the SLM. Subsequently, converging/refocusing is done on only the modulated light through the PRFL, as illustrated in Fig. 3. Although this method increases the control complexity of the SLM, it reduces the complexity of tracking the beam.

As for the diffraction pattern, the implementation of the PRFL changes the shape, intensity, and pattern of the steered beam and diffraction. This can be estimated analytically. The array of pixels shown in Fig. 2 defines the pixel width as s at a lateral distance d along the x axis and with an amplitude after reflection of A. The phase shift induced by this pixel is $\phi = \phi_p + \phi_L$. The modulated field immediately after reflection, $E_m(x_m)$, is approximated by a rectangular function Π:

$$E_m = \sum_{p=1}^{P} A\Pi\left(\frac{x_m - d_p}{s}\right) e^{j\phi_p} e^{j\phi_L}. \tag{1}$$

Equation (2) is used to describe the pixelated phase ramp in Fig. 2, assuming the phase difference and the distance between each pixel are constant:

$$\phi_p = \Delta\phi_p p = \frac{\Delta\phi_r}{P} p\ ,\ d_p = sp. \tag{2}$$

For the Fresnel lens, visually shown in Fig. 2, with Fresnel approximation in 1D:

$$\phi_L = -\frac{k}{2f}x^2 = -\frac{k}{2f}s^2p^2, \tag{3}$$

where f is the focal length and k is the wavenumber. It is convenient to use the Fresnel diffraction for propagation in the near field as the exponential term, i.e., the quadratic phase term across the pupil $\exp\left(jkx_m^2/2z\right)$ cancels out the Fresnel lens phasor at the focal length f. Note that this cannot be done when considering the pixelation; hence, only the ramp phasor is propagated pixelated. Inserting Eq. (1) into the Fresnel diffraction equation and setting the propagation distance $z = f$ yields the following:

$$\begin{aligned} E_f &= \frac{e^{jkf}}{j\lambda f} e^{j\frac{k}{2f}x_f^2} \\ &\int \sum_{p=1}^{P} A\Pi\left(\frac{x_m - d_p}{s}\right) e^{j\phi_p} e^{-j\frac{k}{2f}x_m^2} e^{j\frac{k}{2f}x_m^2} e^{-j\frac{k}{f}x_f x_m} dx_m \\ &= \frac{As}{j\lambda f} e^{jkf} e^{j\frac{k}{2f}x_f^2} \operatorname{sinc}\left(\frac{ks}{2f}x_f\right) \sum_{p=1}^{P} e^{j\left(\phi_p - \frac{2\pi}{\lambda f}x_f d\right)}. \end{aligned} \tag{4}$$

Using the geometric identity,

$$s_n = \sum_{k=0}^{n-1} ar^k = \sum_{k=1}^{n} ar^{k-1} = a\left(\frac{1-r^n}{1-r}\right). \tag{5}$$

When $\phi_p = \Delta\phi_r/Pp$, $r = \exp j\left(\Delta\phi_r/P - 2\pi x_f s/(\lambda z)\right) \neq 1$, $p = k-1$, $n = P$, and $a = 1$, Eq. (4) simplifies to the following:

$$E_f = \frac{1}{j\lambda f} e^{jkf} e^{j\frac{k}{2f}x_f^2} \underbrace{As\operatorname{sinc}\left(\frac{ks}{2f}x_f\right)}_{\text{Amplitude Envelope}} \underbrace{\left(\frac{1 - e^{j\left(\frac{\Delta\phi_r}{P} - \frac{k}{f}sx_f\right)P}}{1 - e^{j\left(\frac{\Delta\phi_r}{P} - \frac{k}{f}sx_f\right)}}\right)}_{\text{Diffraction}}. \tag{6}$$

This equation does not include diffraction from gaps between the pixels, pixelation of the Fresnel lens, and discrepancies in the phase command and output as well as missing spatial dimensions. Nevertheless, the result is plotted in Fig. 4 and shows a pattern formed in the focal plane which follows an amplitude envelope. The steered spot is well defined and simple to track, making the PRFL compatible with criterion 1. Furthermore, the diffraction pattern is spaced apart which allows for the steered beam to be imaged alone on the detector as illustrated in Fig. 4. As a result, the influence of the diffraction pattern on tracking and cross talk can be reduced using the PRFL, which together with NMB amplitude reduction, would make it compatible with criterion 3.

To verify these conclusions and asses the tracking error performance of the PRFL compared to the PR in the presence of the NMB and diffraction for criterion 2, an experiment was conducted. The setup, including components and dimensions, is illustrated in Fig. 5. The beam was aligned with the optical axis when a 0°PRFL was displayed on the SLM. The perfboard is used to create a small beam from a larger collimated beam to simulate an homogeneously illuminated finite aperture.

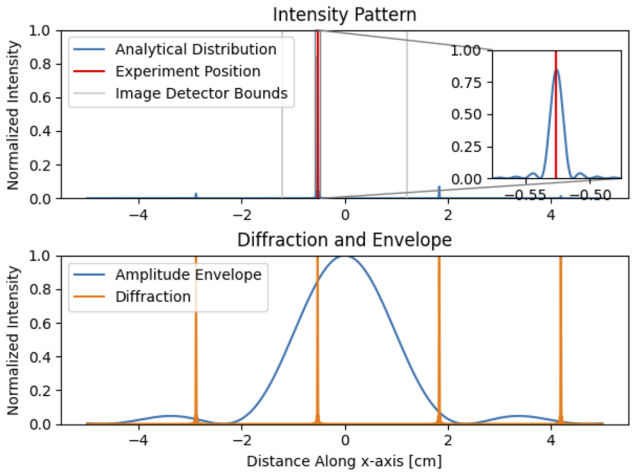

Fig. 4. Results of the analytical approximation of the PRFL in the focal plane. (a) Plot of an output pattern and comparison to the position detected in the experiment ("Experiment Position") for verification. The experiment will be explained later. For clarity, a zoom of the steered beam as well as the image detector bounds is provided. (b) Decomposition of the diffraction pattern in a diffraction pattern and an amplitude envelope to help illustrate the behavior.

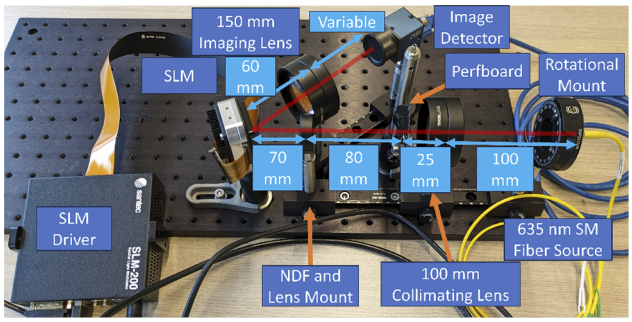

Fig. 5. Labeled image of the experimental setup. The SLM and image detector used are the uncoated SLM-200 and MER2-160-227U3M, respectively [10,11].

The setup allowed for deliberate defocus and focusing by varying the imaging lens distance to the image detector. The image detector exposure time was set to 20 μs. Lastly, the constant position of the zeroth order and NMB allowed for masking in the same position. An illustration of masking is shown in Fig. 6.

Three settings were chosen to assess the suitability of the PRFL according to the criterion mentioned above:

(1) **PR**: to show this method is sensitive to incorrectly track the NMB and diffraction instead of the steered beam without masking.
(2) **PR with the NMB and zeroth order masked**: for a tracking baseline to assess criterion.
(3) **Defocus with the PRFL and no mask**: it verifies the works of the PRFL and its ability to meet criteria 1 and 3.

Beam tracking is done in two stages. The beam is first coarsely tracked using peak intensity and subsequently refined using the local CG. The steps are shown in Fig. 7.

The CG error propagation was analyzed as a way to compare the tracking performance of the PRFL and PR. The norm of the

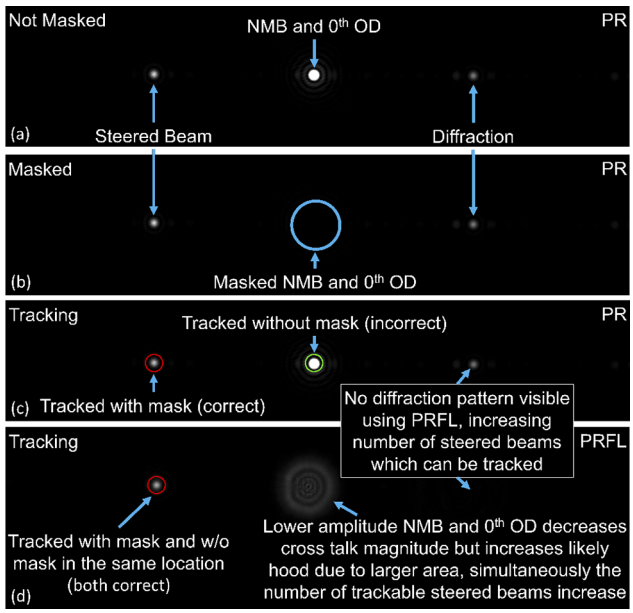

Fig. 6. Figures (a)–(d) show differences in tracking when using the PR and PRFL. These are real images captured during the experiment. (a) Labeled image of a steered beam. "Zeroth-order diffraction" is abbreviated to "0th OD." (b) Demonstration of digital masking; the blue circle shows where the mask is placed. When the mask is applied, all the masked pixels are ignored. (c) Algorithm tracking when using the PR without masking, shown in the green circle, tracks the NMB and 0th OD and not the steered beam due to higher peak intensity. When masking, the correct beam is tracked, shown in red. (d) Algorithm tracking beams when using the PRFL does not require masking; the red and green circles coincide (with the green circle underneath the red circle). Additional benefits of the PRFL are mentioned in the figure.

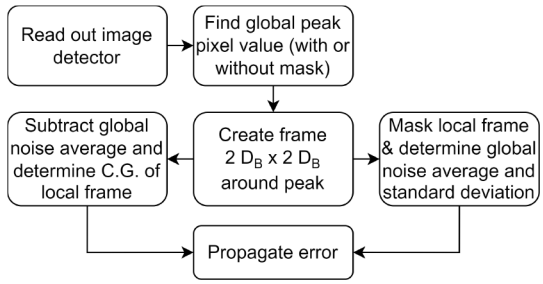

Fig. 7. Spot tracking flow chart. The tracking algorithm uses a peak intensity-informed local CG algorithm as well as error estimation steps. D_g denotes the beam diameter.

signal error vector, Δr_{cgs}, is determined using the following:

$$\Delta r_{cgs} = \Delta r + \frac{\Delta I + \Delta I_{nav}}{\sum_i^N I_{si}} \sum_j^N \left| r_j - r_{cgs} \right|, \tag{7}$$

where Δr, ΔI, and ΔI_{nav} are the offset errors of the pixel position, the pixel value, and the noise average, respectively. The number of pixels in the local frame is denoted by N. The norm of the position vector of the signal CG, r_{cgs}, is the absolute distance from the origin in the local frame. Position norm is defined as $r = \sqrt{x^2 + y^2}$ with x and y denoting the coordinates along their respective axis. The value of pixel i is denoted as I_i and average noise level as I_{nav}, and the CG position is denoted as r_{cgnav} and

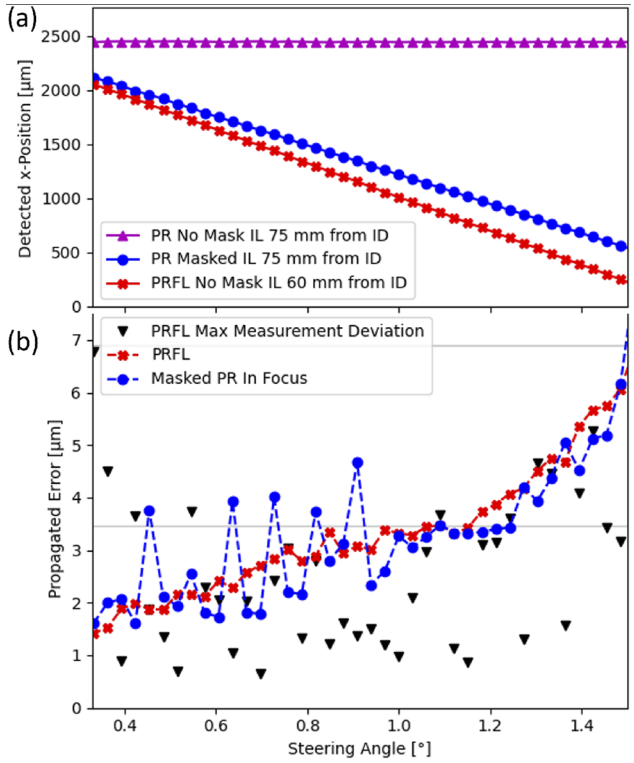

Fig. 8. (a) Relation between the steering angle and detected x-positon for the PR and PRFL. The distance from the imaging lens (IL) to the image detector (ID) changes between PRFL and PR runs and changes the perceived angle. (b) Estimated error together with the maximum measurement deviation from the average detected CG at each beam position. The gray lines indicate one pixel [11].

resides in the center of the local frame. The pixel position error, Δr, was set to 0 as it was assumed that the pixel location error is negligible. ΔI was taken to be the 8-bit discretization of the pixel which is 1 out of 2^8 for the MER2-160-227U3M [11]. Finally, ΔI_{nav} was set to $\sigma_n/\sqrt{N}$, where the standard deviation of the noise, σ_n, is taken from the whole image after the NMB and MB pixels have been masked and ignored. Note that this includes the diffracted light. The variables are assumed to be independent. The beam diameter was determined by finding the intersection between the beam and the noise floor once at the start.

The error propagation results in Fig. 8(b) show that the tracking performance of the masked PR can be met without a mask using the PRFL, meeting criterion 2. From example images in Fig. 6, it can also be observed that the NMB and diffraction for the PRFL is less dominant than for the PR, satisfying criterion 3. Figure 6 and Fig. 8(a) also show that tracking can be performed purely through peak intensity and CG tracking, satisfying criterion 1. Having met all the criteria, the PRFL has the prospect of being a suitable candidate for use in multi-beam steering systems.

The results demonstrate that the PRFL could be particularly effective when the NMB and diffraction are dominant over the signal. Due to no additional hardware components being needed to implement the PRFL, the cost of implementation can be minor. Furthermore, not needing masking or filtering algorithms could make tracking non-static beams using the PRFL easier and more reliable. Lastly, less artifacts to track could also increase the number of beams the system can track.

For SLMs that reduce the NMB by an AR coating, the PRFL could seem to be less relevant. Still the PRFL can further reduce the amount of cross talk originating from the NMB leaking into the wrong comms channel, at the cost of a higher probability of cross talk due to an increased NMB area (discussed in Fig. 6). Other aspects that form a limitation in applying the PRFL are as follows: 1) the limited spatial resolution of the SLM limits the steering angle and the minimum focal length of the FL; 2) computational load and modeling complexity of synthesizing multiple FLs is increased; and 3) for long focal lengths, the effects are reduced.

In conclusion, this paper showed the theory and experimental demonstration of the phase ramp and Fresnel lens (PRFL)-based steering. It shows that deliberate defocus followed by a PRFL phase screen on an SLM in a non-modulated beam (NMB) reflection and diffraction dominant system allows for simple peak intensity tracking and local CG tracking methods without loss of tracking performance or additional hardware. While phase ramp steering required filtering to track, the PRFL was impervious.

When transitioning to multiple beams, the principles will remain the same. However, several practical limitations should be addressed in future research. Given a required minimum number of pixels to implement the PRFL for each beam, the number of beams that can be accommodated in an SLM is limited. Furthermore, the multiple beam tracking algorithm would be different from the algorithm demonstrated in this work.

As a result of potential tracking and cross talk benefits, we believe that the PRFL has good prospects of improving the performance of multi-beam laser communication systems.

Funding. Nederlandse Organisatie voor Wetenschappelijk Onderzoek (P19-13).

Acknowledgment. We are grateful to FREE project (P19-13) of the TTW-Perspectief research program, which is partially financed by the Dutch Research Council (NWO).

Disclosures. The authors declare no conflicts of interest.

Data availability. Data underlying the results presented in this paper are not publicly available but may be obtained from the authors upon reasonable request.

REFERENCES

1. J. J. Spaander, "Free-space multi-beam optical communication terminal design for spacecraft," Master's thesis (Delft University of Technology, 2021).
2. I. Erteza, "Diffraction efficiency analysis for multi-level diffractive optical elements," Tech. Rep. SAND95-1697 (Sandia National Laboratory, 1995).
3. C. J. Henderson, Opt. Eng. **44**, 075401 (2005).
4. X. Deng, C. I. Tang, C. Luo, *et al.*, Micromachines **13**, 966 (2022).
5. D. Engstrom, J. Bengtsson, E. Eriksson, *et al.*, Opt. Express **16**, 18275 (2008).
6. I. Moreno, B. K. Gutierrez, M. M. Sánchez-López, *et al.*, Opt. Lasers Eng. **126**, 105910 (2020).
7. R. S. Ketchum and P. A. Blanche, Photonics **8**, 62 (2021).
8. Z. Wang, C. Wang, S. Liang, *et al.*, Opt. Express **30**, 7319 (2022).
9. J. R. Lindle, A. T. Watnik, and V. A. Cassella, Appl. Opt. **55**, 4336 (2016).
10. "Reflective spatial light modulator (standard model) SLM-200," Santec Holdings, https://www.santec.com/en/products/components/slm/slm-200/.
11. "Mer2-160-227u3m," Daheng Imaging, https://en.daheng-imaging.com/show-106-1968-1.html.